

Electrochemical Behavior of Carbon Steel pre-Treated with an Organo Functional bis-Silane Filled with Copper Phthalocyanine

Patricia H. Suegama and Idalina V. Aoki*

Departamento de Engenharia Química, Escola Politécnica, Universidade de São Paulo, CP 61548,
05424-970 São Paulo-SP, Brazil

Neste trabalho, depositou-se sobre aço carbono o filme de bis-[trimetoxisililpropil]amina (BTSPA) adicionado de ftalocianina de cobre (Cu-Ph). Na obtenção desse filme variou-se as concentrações de Cu-Ph e a temperatura de cura (120 e 150 °C) e nas amostras curadas à 150 °C, adicionou-se uma segunda camada. O comportamento eletroquímico do aço carbono recoberto com o filme aditivado com Cu-Ph foi estudado por técnicas eletroquímicas (medidas de espectroscopia de impedância eletroquímica e curvas de polarização) em solução aerada de NaCl 0,1 mol L⁻¹. A caracterização física e química foi feita por análise termogravimétrica (TGA), microscopia eletrônica de varredura, medidas de ângulo de contato e espectroscopia de infravermelho. A TGA não mostrou decomposição da Cu-Ph durante o processo de cura e a quantidade de Cu-Ph adicionada ao filme polissilânico apresentou forte influência na resistência à corrosão, principalmente quando a amostra é curada a 150 °C. Os resultados mostraram que menores concentrações de inibidor forneceram maior resistência à corrosão e a segunda camada aumentou em uma ordem de grandeza a resistência à corrosão.

The bis-[trimethoxysilylpropyl]amine (BTSPA) film filled with copper phthalocyanine (Cu-Ph) was prepared by adding different concentrations of copper phthalocyanine – Cu-Ph and deposited on a carbon steel substrate using 120 °C and 150 °C as curing temperatures. For samples cured at 150 °C a second layer was also deposited. The electrochemical behavior of carbon steel coated with BTSPA filled with Cu-Ph was studied by electrochemical measurements, electrochemical impedance spectroscopy (EIS) and polarization curves, in aerated 0.1 mol L⁻¹ NaCl solution. Physical and chemical characterization was made by thermogravimetric analysis (TGA), scanning electron microscopy, contact angle measurements and infrared spectroscopy. TGA showed no decomposition of Cu-Ph during the curing process. Cu-Ph added into the silane film showed a strong influence on its corrosion resistance, mainly when the samples are cured at 150 °C. The results showed that lower inhibitor concentrations led to a higher corrosion resistance and the second layer increased by one order of magnitude the corrosion resistance.

Keywords: corrosion, silane film, BTSPA, inhibitor

Introduction

Coupling agents are defined as materials that improve the adhesive bonds of dissimilar surfaces by increasing the interfacial adhesion, improving properties such as wettability, rheology, abrasion and catalytic inhibition, and strengthening of the boundary layers.¹

Organofunctional silanes are hybrid organic-inorganic compounds that can be used as coupling agents across organic-inorganic interface.² They may be used as adhesion

promoters between organic polymers and mineral substrates under a variety of circumstances. The silane adhesion promoters, or “coupling agents”, may function as (i) a finish or surface modifier, (ii) a primer or (iii) an adhesive, depending on the thickness of the bonding material at the interface. A surface modifier or “finish” may theoretically be only a monomolecular layer, but in practice, may be several layers thick.²

Silane coatings are “passive” organic coatings, since they act essentially as a physical barrier that hinders the penetration of aggressive species towards the metallic substrate. However, this behaviour can be

*e-mail: idavaoki@usp.br

modified by the inclusion of small amounts of chemicals with corrosion inhibiting properties.^{1,2} Various organo functional silanes are available in the market today. Applied on different metallic substrates (as zinc,^{3,4} steel,⁵⁻⁷ aluminum,^{3,8,9} magnesium alloy¹⁰), they have been widely studied from both formation and performance points of view.¹¹

A functional bis-silane, $X_3Si-Y-SiX_3$, is a compound where Y is a hydrocarbon chain which can also include a functional group. These silanes are hydrolyzed in a water/alcohol mixture in which a sufficient number of silanol groups (Si-OH) are readily formed. These hydrophilic silanol groups are adsorbed when in contact with a clean metal surface leading to the formation of metallo-siloxane bonds.^{13,14}

One of the ways to increase the corrosion performance of these silanes is to add corrosion inhibitors to the film, which can leach out slowly.

Ferreira *et al.*¹⁵ investigated silane and rare earth salts as chromate replacers for pre-treatments on galvanised steel and showed the two-step (immersion in rare earth followed by immersion in bis-[triethoxysilylpropyl]tetrasulphide - BTESPT) pre-treatments resulted in good protection against corrosion. However, the best performance was obtained with lanthanum conversion coatings. This was observed either on uncoated and paint coated substrates. Silane (BTESPT) itself also showed some improved corrosion protection.

W. Trabelsi *et al.*¹² studied the "passive" barrier properties of silane (BTESPT) coatings through doping with cerium nitrate or with zirconium nitrate. They showed that pre-treatments for galvanized steel substrates, based on BTESPT doped with amounts of cerium nitrate or zirconium nitrate, are much more protective than those based on non-modified silane solutions. The beneficial effects of cerium are more important than those of zirconium.

V. Palanivel *et al.*¹³ studied the effects of addition of corrosion inhibitors (tolyltriazole, benzotriazole and cerium nitrate) to silane films in the performance of AA2024-T3 with 0.5 mol L⁻¹ NaCl. They showed that silane films when loaded with organic or inorganic inhibitors also present the property of protecting fresh exposed metal. Silane films acted as inhibitor reservoir and released them into the solution where they migrated to damaged areas and protected metal from corrosion.

Organic corrosion inhibitors are promising candidates, as they appear to be easily compatible with hybrid coating material that can be loaded with inhibitors by adding the inhibitor into the hydrolysis solution prior to cross-linking and film formation. Corrosion inhibitors trapped within the coating material are leachable and active in the corrosive

environment, making this doping procedure a simple and effective process for inhibitor storage and release.¹⁶

Aoki *et al.*¹⁷ verified the efficiency of copper phthalocyanine as a corrosion inhibitor for ASTM A606-4 steel in 16% hydrochloric acid, as well as, the degree of protection. Electrochemical measurements showed slight changes in open circuit potential and polarization curves showed that copper phthalocyanine acts as a mixed inhibitor for steel, and EIS measurements showed that inhibitor's efficiency is observed for increasing copper phthalocyanine (Cu-Ph) concentrations.

The purpose of this study is to verify the influence of an inhibitor (copper phthalocyanine) concentration in a bis-[trimethoxysilylpropyl]amine (BTSPA) film by electrochemical methods and to characterize the film morphological and chemically in order to determine if this inhibitor can be used in association with the silane film in order to provide corrosion protection properties for carbon steel substrate.

Experimental

UNS 10100 steel with a nominal composition of 0.1 wt.% C, 0.30 wt.% Mn, 0.05 wt.% S, 0.04 wt.% P and balance of Fe was used as substrate. The steel substrate was degreased using an acetone ultrasonic bath for 10 min and then immersed in a 2.5% m/m NaOH solution also for 10 min. The alkaline treatment helps to improve the wettability of the metallic substrate and to obtain a water break-free surface. Following alkaline treatment, the panels were rinsed with distilled water/ethanol or ketone and dried in a hot air stream.¹⁸

In an ethanol/deionised water (50/50) solvent at pH 4.0 (adjusted with acetic acid) the bis-[trimethoxysilylpropyl]amine (BTSPA) (Figure 1A) was added forming a solution (2% m/m silane / 98% m/m solvent). It is worthy to stress the large water amount employed in the silane hydrolysis. The solution was stirred at room temperature for 30 min to allow hydrolysis occur. Copper phthalocyanine (Figure 1B) inhibitor was dissolved in the ethanol/deionised water solvent before the silane addition. Three groups of samples were obtained: (i) one immersion in hydrolysis solution (with Cu-Ph) and curing at 120 °C for 40 min; (ii) one immersion in hydrolysis solution (with Cu-Ph) and curing at 150 °C for 40 min; (iii) one immersion in hydrolysis solution (with Cu-Ph) and curing at 150 °C for 20 min, followed by another immersion in hydrolysis solution (without Cu-Ph) and curing at 150 °C for 40 min.

All the conditions employed are in Table 1, where S = single layer, D = double layer; 120 or 150 are curing temperatures; and letters from A to D = increasing Cu-Ph

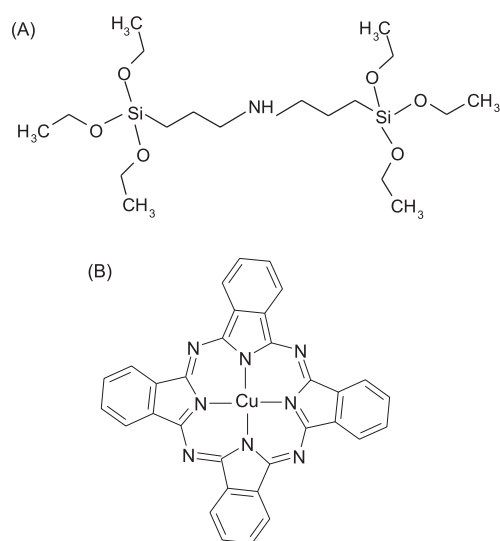


Figure 1. Schematic molecular structures of (A) bis-[trimethoxysilylpropyl] amine (BTSPA) and (B) copper phthalocyanine (Cu-Ph).

concentration. The copper phthalocyanine concentrations used in this study were: (A) 1×10^{-4} , (B) 5×10^{-4} , (C) 1×10^{-3} and (D) 5×10^{-3} mol L⁻¹ and F = BTSPA film without Cu-Ph.

TGA analysis was performed in an oxidative atmosphere (air) with a linear temperature ramp. The maximum temperature was 800 °C, 10 °C min⁻¹ heating rate and samples of approximately 10 mg were used.

Contact angle was determined by the sessile drop method using a Ramé-Hart contact-angle goniometer, Model 100-10. Several measurements were carried out in the substrate with a water drop of ca. 15 mm³ under room atmosphere.

Surface characterization was made by a Philips XL-30 scanning electron microscope (SEM) coupled to an energy dispersive spectrometer analyzer (EDS). FTIR-RA measurements were obtained using a Bomem MB 100 spectrophotometer in the range from 4000 to 400 cm⁻¹ with a spectral resolution of 4 cm⁻¹.

Corrosion resistance of the coated steel was evaluated by electrochemical measurements of the samples in 400 mL of aerated and unstirred 0.1 mol L⁻¹ NaCl solution. An Ag|AgCl|KCl_{sat} electrode, connected to the working solution through a Luggin capillary, was used as reference and a Pt network as auxiliary electrode. Finally, a working electrode of each coated panel was mounted in the EG&G electrochemical flat cell, exposing an area of 1 cm² to the solution.

Electrochemical impedance (EIS) measurements were made using EG&G Parc-283 potentiostat and a frequency response analyzer Solartron-SI1255. The EIS tests were performed applying 10 mV (rms) to the stationary E_{oc} value, starting from 5×10^4 to 5×10^{-2} Hz and 7 measurements per frequency decade. Polarization curves were recorded for all samples in a potential range from -250 to +250 mV versus E_{corr}/Ag|AgCl|KCl_{sat} at 0.5 mV s⁻¹ scan rate.

Results and Discussion

Reagent characterization

Thermogravimetric analysis (TGA) is an analytical technique used to determine a material's thermal stability and its fraction of volatile components by monitoring the

Table 1. Conditions employed and parameters for coated steel samples

Sample	Immersion time in [Cu-Phcy]+ BTSPA hydrolysis solution	[Cu-Phcy] / (mol L ⁻¹)	1 st Cure Temperature/ time	Immersion time in BTSPA hydrolysis solution	2 nd Cure Temperature/ time
S120A	2 min	1×10^{-4}	120 °C/40 min	-----	-----
S120B	2 min	5×10^{-4}	120 °C/40 min	-----	-----
S120C	2 min	1×10^{-3}	120 °C/40 min	-----	-----
S120D	2 min	5×10^{-3}	120 °C/40 min	-----	-----
S120F	2 min	-----	120 °C/40 min	-----	-----
S150A	2 min	1×10^{-4}	150 °C/40 min	-----	-----
S150B	2 min	5×10^{-4}	150 °C/40 min	-----	-----
S150C	2 min	1×10^{-3}	150 °C/40 min	-----	-----
S150D	2 min	5×10^{-3}	150 °C/40 min	-----	-----
S150F	2 min	-----	150 °C/40 min	-----	-----
D150A	2 min	1×10^{-4}	150 °C/20 min	2 min	150 °C/40 min
D150B	2 min	5×10^{-4}	150 °C/20 min	2 min	150 °C/40 min
D150C	2 min	1×10^{-3}	150 °C/20 min	2 min	150 °C/40 min
D150D	2 min	5×10^{-3}	150 °C/20 min	2 min	150 °C/40 min
D150F	2 min	-----	150 °C/20 min	2 min	150 °C/40 min

weight change that occurs as a specimen is heated. It is commonly employed in research and testing to determine characteristics of materials such as polymers, to determine degradation temperatures, absorbed moisture content of materials, level of inorganic and organic components in materials, decomposition points of explosives, and solvent residues. It is often used to estimate corrosion kinetics in high temperature oxidation. This technique measures changes in weight of a sample with increasing temperature. Moisture content and presence of volatile species can be determined by this technique.¹⁹ In order to observe if the Cu-Ph is stable at curing temperature, thermogravimetric analyses (TGA) measurement were done to pure Cu-Ph and pure BTSPA silane and are presented in Figure 2.

Figure 2 shows the stability of Cu-Ph until *ca.* 450 °C, and then the curing temperature is not able to produce its degradation. TGA of BTSPA shows a high decrease of weight at temperature lower than 150 °C, attributed to water loss, in agreement with condensation process to form Si-O-Si bonds. As can be seen, at 100 °C, water not retained into the film is lost, and then a 120 °C temperature was used with the aim to minimize the final process cost and a higher temperature (150 °C) was also studied. Both temperatures were chosen to observe the cost/benefit relation in the crosslinking process.

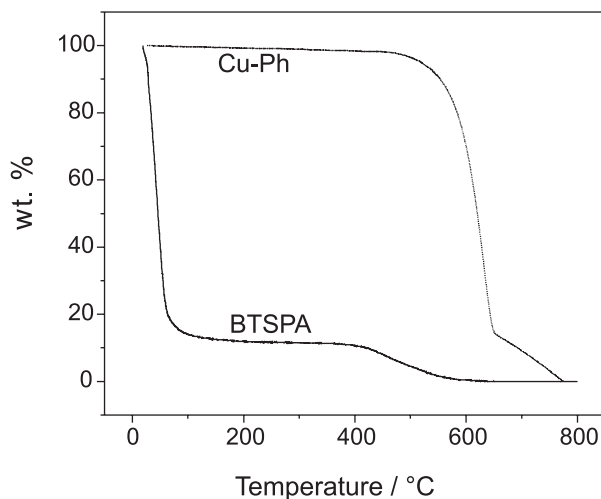


Figure 2. TGA curves of Cu-Ph and BTSPA.

Film characterization

S120F and S120A (lowest Cu-Ph concentration) coated samples FTIR-RA spectra (reflection/absorption Fourier transform infrared spectroscopy) and absorption spectrum for pure Cu-Ph peaks indicate that the characteristic Cu-Ph peaks are not shifted when added to the film as in Figure 3A, indicating that Cu-Ph does not present significant

chemical interaction with the BTSPA, even for higher Cu-Ph concentrations as in S150D sample (Figure 3b). The detailed attribution of peaks of the phthalocyanine skeleton is found in the literature.^{20,21} Cu-Ph particles are dragged by the silane solution that wets the steel surface, and when the sample is cured, ethanol and water volatilize and the copper phthalocyanine is fixed in the lattice formed by the silane reticulation during the curing process.

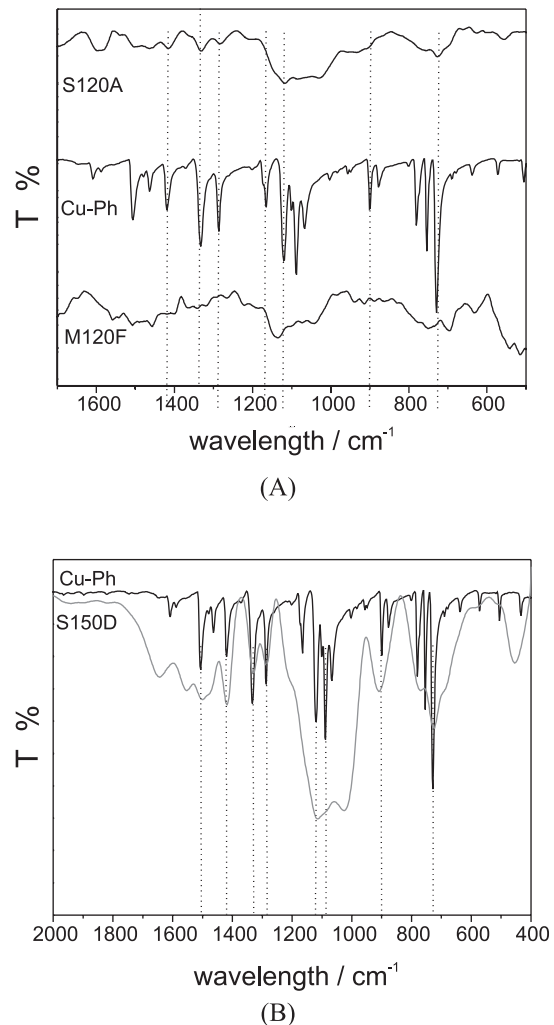


Figure 3. FTIR-RA spectra of (A) S120F, S120A samples and (B) S150D sample and absorption IR spectra of pure Cu-Ph.

Figure 4 presents the absorption IR spectra of pure polymerized BTSPA after curing at 120 °C and 150 °C for 40 min and in Table 2, the main peaks are described. Si-O-Si peaks appear between 1,130-1,000 cm^{-1} and Si-O-H at 900-950 cm^{-1} . A more intense peak at 1,110 cm^{-1} , attributed to SiOSi indicates a denser siloxane network at samples obtained at 150 °C than at 120 °C curing temperature.²⁴ The presence of an intense band in 1,130 cm^{-1} is related with the formation of Si-O-Si bonds that impart to the film a protective effect for the substrate, which can

be observed by EIS measurements. The peak at $1,600\text{ cm}^{-1}$ evidences the presence of the amine group (NH_2) and at $3,600\text{ cm}^{-1}$ a band due to N-H stretching can be observed.

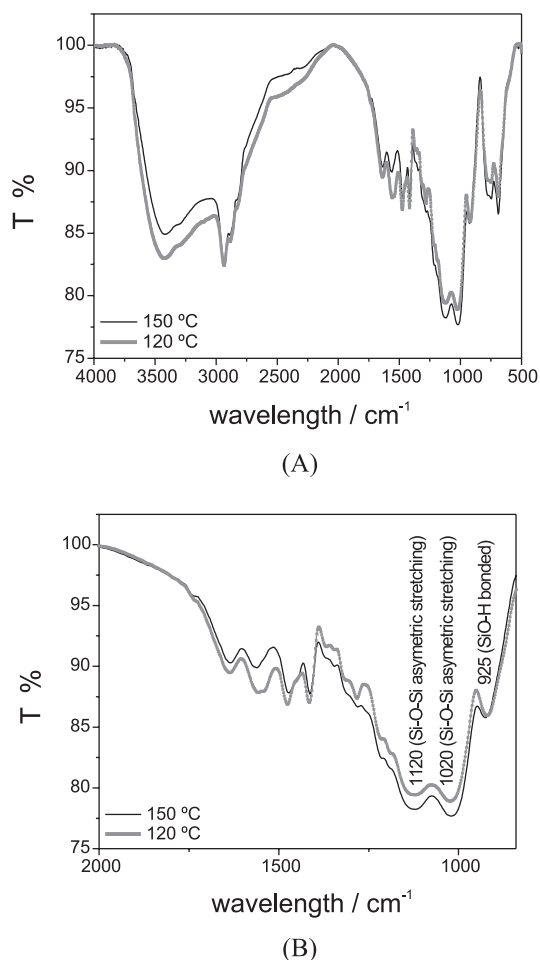


Figure 4. Absorption IR spectra of pure polymerized BTSPA (it is not a film) cured at $120\text{ }^\circ\text{C}$ and $150\text{ }^\circ\text{C}$: (A) from 500 to $4,000\text{ cm}^{-1}$ and (B) from 750 to $2,000\text{ cm}^{-1}$.

Table 2. Absorption region and bond type found in silanes^{21,22}

Wavelength / cm^{-1}	Bond type
700-800	C-H ($\text{Si-CH}_2\text{-CH}_2\text{-Si}$) stretching vibrations
860-760	Si-C stretching
890-920	Si-O (Si-OH) stretching vibrations
900-960	Si-O- C_2H_5 vibrations
1,130-1,000	Si-O-Si asymmetric stretching
1,250-1,200	Si- $\text{CH}_2\text{-R}$ deformation
1,300-1,400	CH_2 and CH_3 bending vibrations
1,575-1,600	N-H (NH_2) bending vibrations
1,700-1,750	C=O (acetic acid) stretching vibrations
2,900-3,000	C-H (CH_2 and CH_3) stretching vibrations
3,200-3,700	OH (from Si-OH group or H_2O) stretching vibrations
3,400-3,700	N-H stretching vibrations

At $2,900\text{ cm}^{-1}$ the peak of C-H stretching (CH_2 and CH_3) can be found.

Figure 4A shows the band at $3,000\text{-}3,500\text{ cm}^{-1}$ which is attributed to O-H bond, that can be related to water, ethanol and/or silanol group, but it is possible to observe a decrease of this band with the increase of the curing temperature, and at $1,000\text{-}1,100\text{ cm}^{-1}$ the reverse can be seen, indicating that there are more Si-O-Si bonds at $150\text{ }^\circ\text{C}$.

The peak at 925 cm^{-1} , in Figure 4B is attributed to remaining Si-O-H group not involved during the reticulation of the silane. It can be seen that the peaks at 925 cm^{-1} for cured film at 120 and $150\text{ }^\circ\text{C}$ present almost equal intensity, as a response with similar effect of temperature and time of curing in the consumption of Si-OH groups, taking into account the small difference between the two curing temperatures for silane films.²⁴

Doublet peaks at $1,350\text{ cm}^{-1}$ and $1,450\text{ cm}^{-1}$ is attributed to the formation of ammonium acetate²⁴ and another doublet at $1,500\text{-}1,600\text{ cm}^{-1}$ is attributed to O-H stretching in the ethanol of solvent. All these peaks diminish in intensity for higher curing temperature indicating the withdrawn of ethanol and water during the film curing besides the formation of COO^- ions by reaction of secondary groups and acetic acid. All these phenomena occur simultaneously, and it is impossible to distinguish them.

Figure 5 shows SEM images of S120A, S120D samples and pure Cu-Ph deposited on substrate. Figure 5A shows a homogeneous surface, where Cu-Ph is dissolved into the film. In Figure 5B, it is possible to observe that Cu-Ph does not interact with the film, being only physically retained on the surface by the silane film. Comparing Figure 5A and 5B, in which a high quantity of copper phthalocyanine is added, it is possible to see that the silane film cannot cover all inhibitor particles and cracks appear in the silane film on the top of Cu-Ph when the sample is submitted to the curing process. Cracks are formed by curing process due to the water/ethanol loss and siloxane bonding formation that stretch out on the surface. These defects in the film for high concentration of Cu-Ph can facilitate the electrolyte permeation and consequently attack the substrate. The same occurred for S150 series.

A possible relation of the protection against corrosion supplied by the film to the substrate can be established with the hydrophobic character of the sample surface. Then, contact angle was measured and obtained data are shown in Table 3 (results are the average value for measurements conducted on different sites of a given coated steel plate).

Contact angle is the angle at which a liquid/vapor interface meets the solid surface. Contact angle is specific for any given system and is determined by interactions

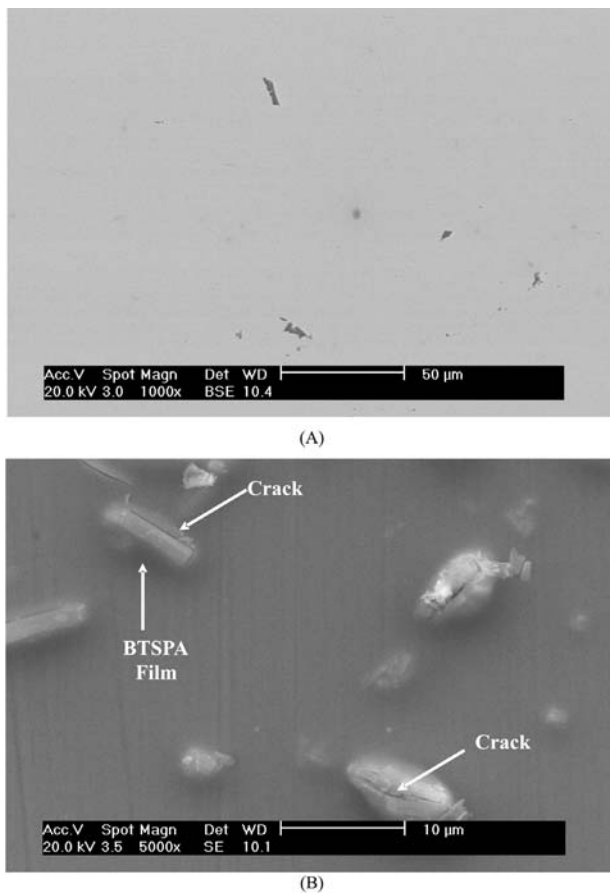


Figure 5. SEM image of (A) S120A, (B) S120D.

Table 3. Results of the contact angle measurements conducted on silane coated carbon steel samples

M120A		M120B		M120C		M120D	
R ¹	L ²	R ¹	L	R ¹	L	R ¹	L
86 ± 1	87 ± 1	79 ± 1	79 ± 1	60 ± 1	60 ± 1	61 ± 1	61 ± 2

¹ = right side; ² = left side.

M150A		M150B		M150C		M150D	
R ¹	L ²						
83 ± 1	81 ± 1	75 ± 1	74 ± 1	70 ± 1	70 ± 1	68 ± 1	69 ± 1

¹ = right side; ² = left side.

D150A		D150B		D150C		D150D	
R ¹	L ²						
76 ± 1	74 ± 1	86 ± 2	85 ± 2	83 ± 1	82 ± 1	70 ± 1	71 ± 1

¹ = right side; ² = left side.

M120F		M150F		D150F	
R ¹	L ²	R ¹	L ²	R ¹	L ²
69 ± 1	69 ± 2	75 ± 1	74 ± 1	75 ± 1	76 ± 1

¹ = right side; ² = left side.

across the three interfaces. A wettable surface may also be termed hydrophilic and a non-wettable surface, hydrophobic.²⁵ On extremely hydrophilic surfaces, a water droplet will completely spread (an effective contact angle of 0°). This occurs for surfaces that have a large affinity with water (including materials that adsorb water). On many hydrophilic surfaces, water droplets will exhibit contact angles from 10° to 30°. On highly hydrophobic surfaces, which are incompatible with water, one observes a large contact angle (70° to 90°). Contact angle thus, directly provides information on the interaction energy between the surface and the liquid.^{25,26} A contact angle of 90° or greater generally characterizes a surface as not-wettable, and angles lower than 90° means that the surface can be wettable at some extent.

Contact angle values for S120 series showed a higher hydrophobicity for samples with lowest copper phthalocyanine concentration, so it was expected that this sample presented a higher barrier effect than did others, promoting a greater corrosion resistance (which was confirmed by electrochemical measurements). Contact angle measurements for S150 and for D150 series showed higher values for samples S150A and D150B, respectively, indicating that these samples present higher hydrophobic surfaces. Comparing the curing process at 120 °C and 150 °C it is possible to observe that samples cured at 150 °C present a higher contact angle values. Contact angle measurements are more sensitive to the number of Si-OH hydrophilic groups on the surface in comparison to IR analysis.

Electrochemical characterization

Electrochemical impedance spectroscopy (EIS) experiments were performed at the stabilized open-circuit potential, E_{oc} . Nyquist plot for bare carbon steel (Figure 6) shows a capacitive semicircle that is close to 2 kΩ and is the lowest value measured among the studied systems.

EIS diagrams of S120 series obtained after 1 h of immersion (data not presented) showed an increase in the inhibitor concentration in the hydrolysis solution reducing the diameter of the capacitive arcs of the silane coated samples; samples with a higher amount of Cu-Ph provided lower protection to the steel substrate due to the presence of cracks in the film caused by the large amount of particles of Cu-Ph retained in the film. Silane coated samples with 1×10^{-4} mol L⁻¹ of Cu-Ph performed much better in terms of corrosion resistance as compared with pure BTSPA film or BTSPA filled with higher Cu-Ph concentrations. The highest total impedance obtained for S120 series was about 12 kΩ, that is lower than the values obtained for S150 and D150 series. Comparing S120 and S150 series, S150

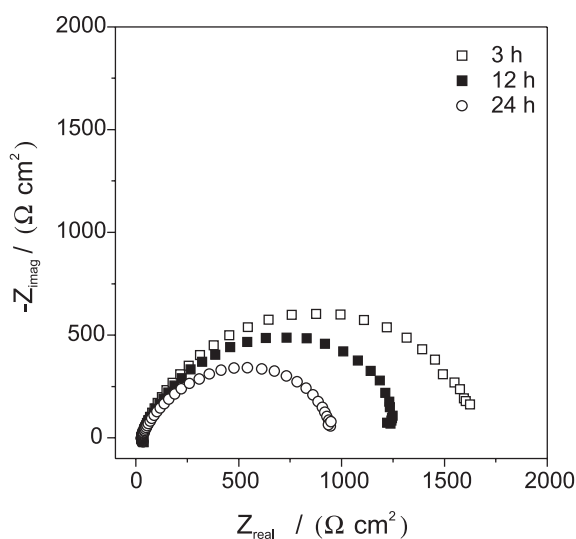


Figure 6. Nyquist plots for carbon steel substrate obtained after 3, 12 and 24 h of immersion in 0.1 mol L⁻¹ NaCl solution.

series presents total resistance higher than S120 series due to a better reticulation of the film at 150 °C, which can be confirmed by IR analysis (more intense peak at 1,100 cm⁻¹ due to Si-O-Si).

Figure 7 shows Nyquist and Bode plots for S150 series after 3, 12 and 24 h of immersion. It can be observed that the polarization resistance and at least two time constants, the first one attributed to the silane film, appears at high frequencies and the second time constant at low frequencies is attributed to the substrate oxidation.

After 3 h immersion, S150A and S150B samples (Figures 7A and 7B) present two well defined time constants and for S150C and S150D samples (Figures 7C and 7D) the constants are overlapped, indicating that these samples can be easily attacked by the electrolyte. S150A and S150B samples show high total impedance for the first 3 h of immersion and a decrease after 12 h and 24 h. High total impedance measured after 3 h immersion should be related to the hydrophobic surface and to the good quality film reticulation formed in the electrode surface as a consequence of higher temperature used in the curing process. For longer immersion times, the total impedance values decreased, probably due to the electrolyte penetration into the film reaching the substrate. These results clearly indicate that the film and its surface, and film/substrate interface degrade as the immersion time increases. This fact can be observed clearly by Bode phase angle plots, in which time constant, attributed to the film, at high frequencies shifts to low frequencies and the second time constant, attributed to the substrate, at low frequencies shifts to

higher frequencies. Bode phase angle plots show that longer immersion time had the maximum increment at intermediary frequencies (*ca.* 1-10 Hz) which is better defined while the one at higher frequency (attributed to the film) almost disappears.

Bode phase angle plots of S150C and S150D samples, do not show a well defined separation between time constants, the constants are already overlapped showing that the electrolyte reach the substrate easily because of cracks created during the curing process.

The sample that presented higher total impedance was S150A followed by S150B > S150C > S150D, indicating that a higher amount of Cu-Ph increases stress and cracks in the film.

Figure 8 shows EIS data for D150 series and the same process observed for S150 series was also observed for D150 series. However, the total impedance increased one order of magnitude and a delay in the electrolyte attack to the substrate was observed to all coated samples. Time shift constants in the Bode phase angle plots were also observed but at lower intensity. D150 series resists more than 72 h with total impedance values higher than 15 kΩ cm², while S150 series after 24 h already presented values lower than 15 kΩ cm². These data indicate the second layer can improve the corrosion resistance and it can be due to the fact that the second layer covers the cracks, decreasing the defects, and/or the second curing process improves a better reticulation of the first layer.

Figure 8 allows observing much higher total impedance values (100 kΩ cm²) than any other series, indicating a better protection provided to the substrate with a double layer of silane when compared to only a single layer. Comparing the capacitive arcs of samples, D150B (Figure 8B) and D150C (Figure 8C) samples presented highest total impedance values after 3 h immersion, and comparing both, D150B presented a larger capacitive arc than did D150C sample. These facts can be attributed to: in D150A sample the inhibitor concentration is very low, then, it lacks for inhibitor; and in D150D sample Cu-Ph concentration is very high, then there are a lot of defects that are not totally coated by the second layer. In D150B and D150C samples, an intermediary inhibitor concentration increases the resistance against chloride ions, because it has enough inhibitor and the second layer minimizes the defects caused by Cu-Ph particles during the curing process.

The second layer covers the first layer, and then it is possible to increase the Cu-Ph concentration into the film, because the second layer will cover the defects, closing the cracks previously present in the first layer.

Figure 9 presents one polarization curve for each condition (samples that presented the best results from each

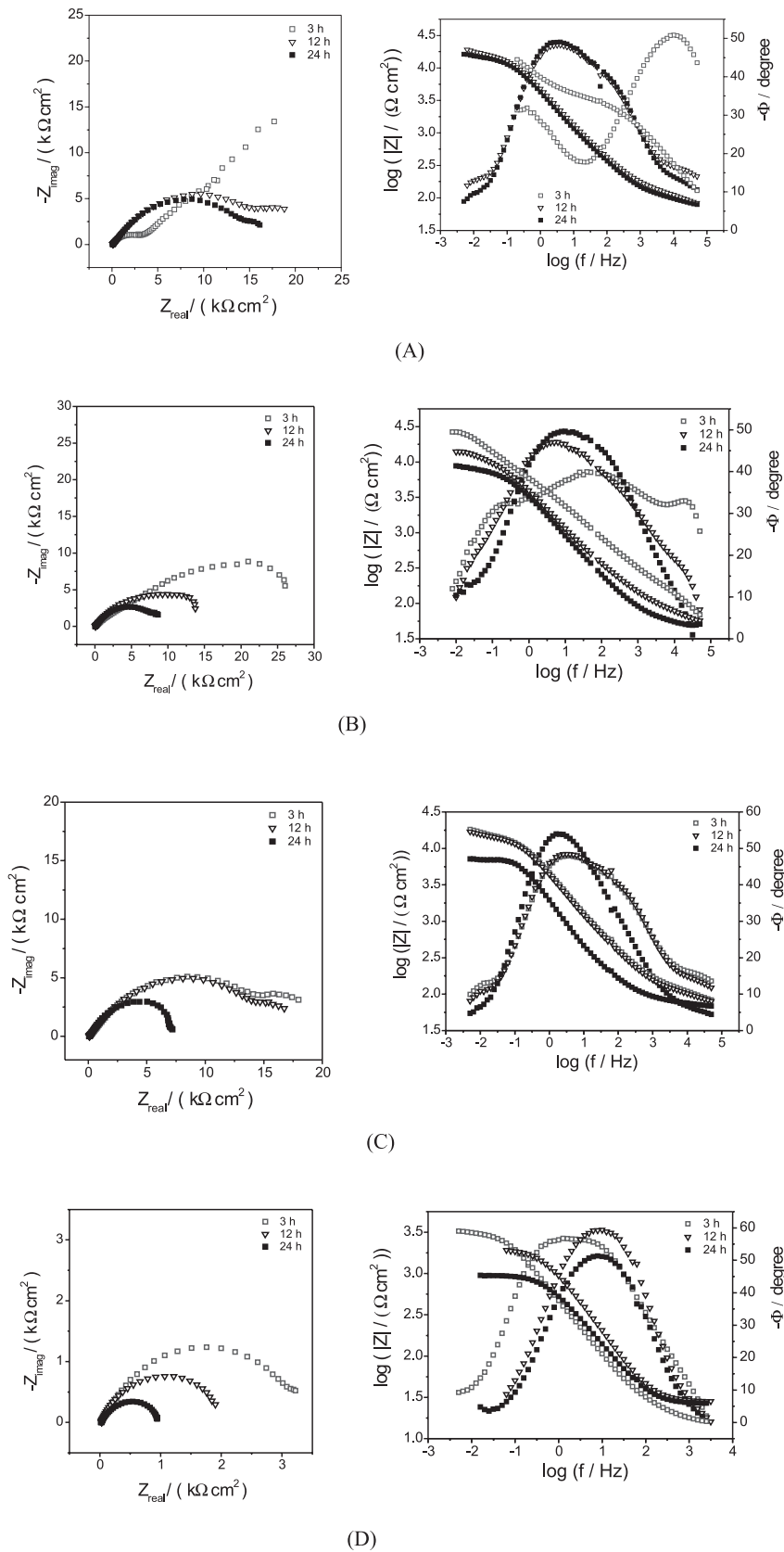


Figure 7. EIS diagrams for S150 series, Nyquist plots and $\log |Z|$ and $-\phi$ vs. $\log(f)$ Bode plots for (A) S150A (B) S150B, (C) S150C and (D) S150C samples obtained after 3, 12 and 24 h of immersion in 0.1 mol L⁻¹ NaCl solution.

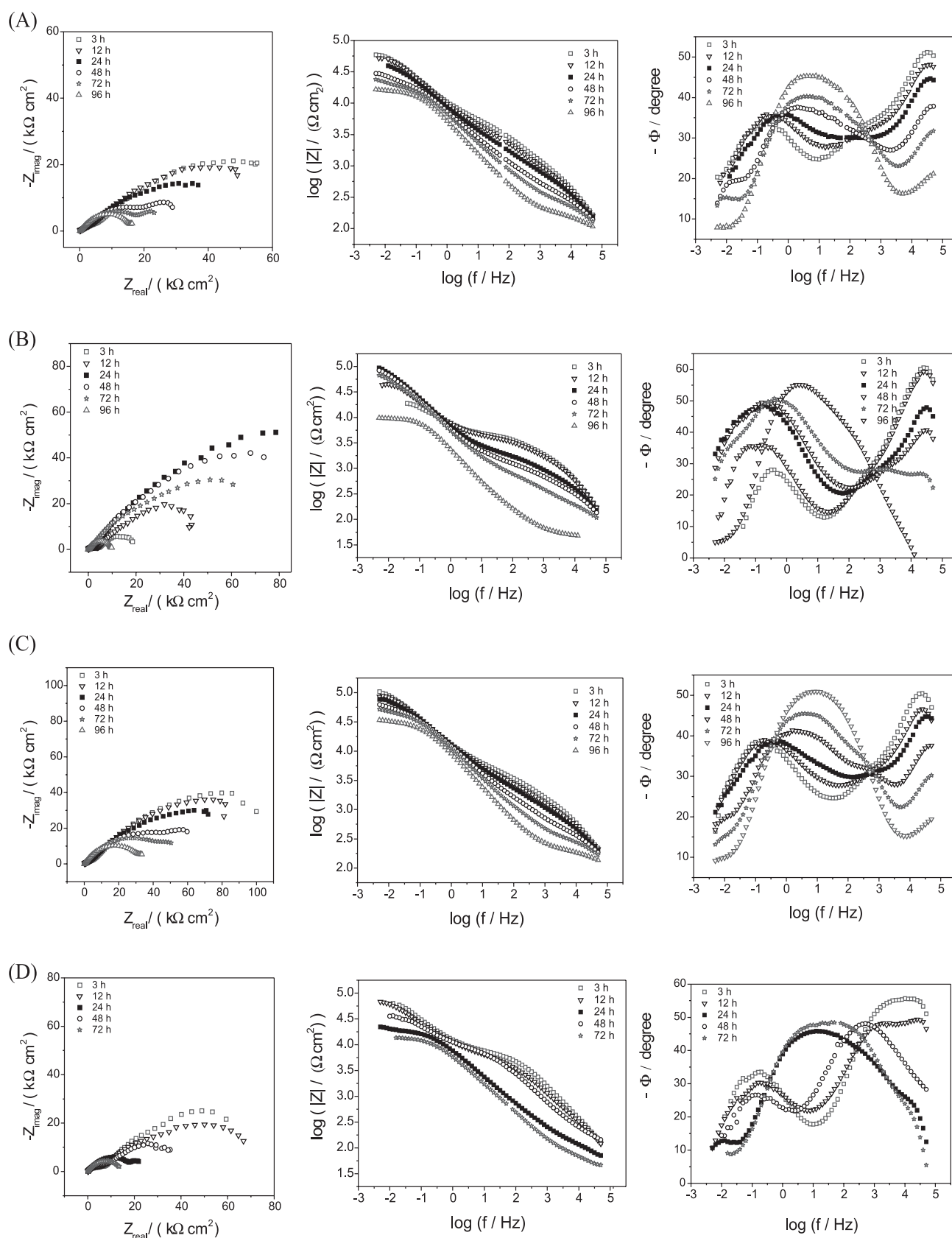


Figure 8. EIS diagrams for D150 series, Nyquist plots and $\log |Z|$ and $-\phi$ vs. $\log(f)$ Bode plots for (A) D50A (B) D150B, (C) D150C and (D) D150D samples obtained after 3, 12, 24, 48, 72 and 96 h (not obtained to D150D) of immersion in 0.1 mol L⁻¹ NaCl solution.

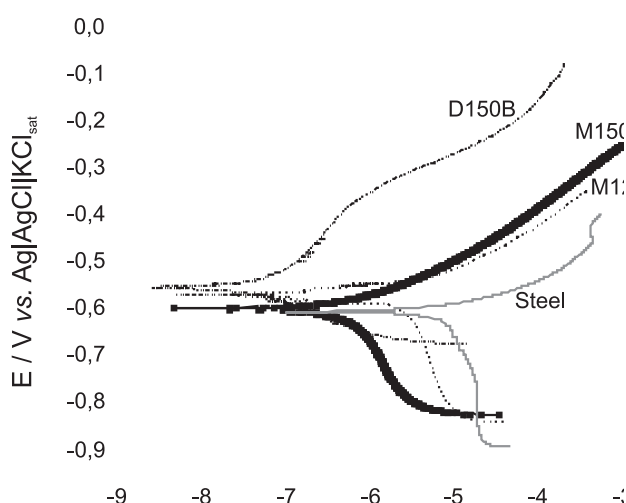


Figure 9. Polarization curves for (A) S120A, (B) S150A and (C) D150B samples obtained after 30 min of immersion in 0.1 mol L⁻¹ NaCl solution at 25 °C and $\nu = 0.5$ mV s⁻¹.

series (S120A, S150A and D150B samples), comparing current density response at -0.4 V, for example, it is possible to observe that D150B sample presented a current density more than two orders of magnitude lower than S120A and S150A samples and three orders of magnitude lower than bare carbon steel substrate, indicating that the polarization measurements can be used to distinguish very good from very bad quality films. Films with similar characteristics present overlapped curves being difficult to interpret and make conclusions. EIS measurements made it possible to better distinguish between good and bad quality films because this technique is more sensitive than the polarization curves. But compared to carbon steel substrate, all samples presented a lower current density response and it represents a protection to substrate.

Conclusions

Temperature of the silane film cure process influences the corrosion protection of substrate. Silane single and double layer can supply protection to the substrate, but when a double layer is used, the corrosion resistance increases by one order of magnitude. Silane films when filled with Cu-Ph provide improved corrosion resistance to the substrate. When a single layer was used, the optimum copper phthalocyanine concentration in the corresponding silane solution was 1×10^{-4} mol L⁻¹. Incorporation of an extra amount of Cu-Ph in to BTSPA film seemed to degrade the corrosion performance of the film. When a double layer is prepared, the first layer can be filled with 5×10^{-4} - 1×10^{-3} mol L⁻¹ concentration of copper phthalocyanine.

EIS results indicated the BTSPA film heavily loaded with Cu-Ph tends to prematurely degrade the film on carbon steel substrate. In double layer films it is possible to increase the Cu-Ph concentration because the second layer close the defects caused by curing process in the first layer.

Incorporation of Cu-Ph into the silane film showed a positive effect on the overall corrosion performance of the coated steel system, mainly for double layer films.

Acknowledgments

The authors are grateful to FAPESP-Fundação de Amparo à Pesquisa do Estado de São Paulo for the postdoctoral scholarship (Proc. no. 05/51851-4).

References

1. Subramanian, V.; *MSc Dissertation*, University of Cincinnati, Cincinnati, US, 1999.
2. Plueddemann, E. P.; *Silane Coupling Agents*, 1st ed., Plenum Press: New York, 1982.
3. Montemor, M. F.; Simões, A. M.; Ferreira, M. G. S.; Williams, B.; Edwards, H.; *Prog. Org. Coat.* **2000**, *38*, 17.
4. Schaftinghen, T. V.; Pen, C. L.; Terryn, H.; Hörzenberger, F.; *Electrochim. Acta* **2004**, *49*, 2997.
5. Subramanian, V.; van Ooij, W. J.; *Corrosion* **1998**, *54*, 204.
6. Wapner, K.; Grundmeier, G.; *Surf. Coat. Technol.* **2005**, *200*, 100.
7. Montemor, M. F.; Rosqvist, A.; Fargerholm, H.; Ferreira, M. G. S.; *Prog. Org. Coat.* **2004**, *51*, 188.
8. Cabral, A.; Duarte, R. G.; Montemor, M. F.; Zheludkevich, M. L.; Ferreira, M. G. S.; *Corros. Sci.* **2005**, *47*, 869.
9. Franquet, A.; Terryn, H.; Vereecken, J.; *Thin Sol. Films* **2003**, *441*, 76.
10. Zucchi, F.; Grassi, V.; Frignani, A.; Monticelli, C.; Trabaneli, G.; *Surf. Coat. Technol.* **2006**, *200*, 4136.
11. Franquet, A.; De Laet, J.; Schram, T.; Terryn, H.; Subramanian, V.; van Ooij, W. J.; *Thin Sol. Films* **2001**, *384*, 37.
12. Trabelsi, W.; Dhouibi, L.; Ferreira, M. G. S.; Zheludkevich, M. L.; Montemor, M. F.; *Surf. Coat. Technol.* **2006**, *200*, 4240.
13. Palanivel, V.; Huang, Y.; van Ooij, W. J.; *Prog. Org. Coat.* **2005**, *53*, 153.
14. Zhu, D.; van Ooij, W. J.; *Corros. Sci.* **2003**, *45*, 2177.
15. Ferreira, M. G. S.; Duarte, R. G.; Montemor, M. F.; Simões, A. M. P.; *Electrochim. Acta* **2004**, *49*, 2927.
16. Khramov, A. N.; Voevodin, N. N.; Balbyshev, V. N.; Mantz, R. A.; *Thin Sol. Films.* **2005**, *483*, 191.
17. Aoki, I. V.; Guedes, I. C.; Maranhão, S. L. A.; *J. Appl. Electrochem.* **2002**, *32*, 915.
18. Trabelsi, W.; Dhouibi, I.; Triki, E.; Ferreira, M. G. S.; Montemor, M. F.; *Surf. Coat. Technol.* **2005**, *192*, 284.

19. Brown, M. E.; *Introduction to Thermal Analysis, Techniques and Applications*, 2nd ed., Kluwer Academic Publishers: New York, 2001.
20. Lever, A. B. P.; *Adv. Inorg. Chem. Radiochem.* **1965**, 7, 27.
21. Maranhão, S. L. A.; Guedes, I. C.; Anaissi, F. J.; Toma, H. E.; Aoki, I. V.; *Electrochim. Acta* **2006**, 52, 519.
22. Silverstein, R. M.; Webster, F. X.; Kiemle, D.; *Spectrometric Identification of Organic Compounds*, 7th ed., John Wiley & Sons: New York, 2005.
23. Stuart, B.; *Modern Infrared Spectroscopy*, 1st ed., John Wiley & Sons: New York, 1996.
24. van Ooij, W. J.; Zhu, D.; Palanivel, V.; Lamar, J. A.; Stacy, M.; *Silicon Chem.* **2006**, 1-2, 11.
25. Hiemenz, P. C.; Rajagopalan, R.; *Principles of Colloid and Surface Chemistry*, 3rd ed., Marcel Dekker: New York, 1997.
26. Lyklema, J.; van Leeuwen, H. P.; *Fundamentals of Interface and Colloid Science*, Elsevier Academic Press: The Netherlands, 1991.

Received: September 30, 2007

Web Release Date: April 29, 2008

FAPESP helped in meeting the publication costs of this article.